ELSEVIER

S0966-9795(96)00058-1

Intermetallics 4 (1996) 601–611

0966-9795/96/$15.00

Grain boundary self-diffusion of ^{63}Ni in pure and boron-doped Ni_3Al

S. Frank, J. Rüsing* & Chr. Herzig

Institut für Metallforschung, Universität Münster, Wilhelm-Klemm-Str. 10, D-48149 Münster, Germany

(Received 11 March 1996; accepted 26 March 1996)

Grain boundary (gb) self-diffusion in pure Ni-rich Ni_3Al was measured between 882 and 1374 K using the radiotracer ^{63}Ni, a serial sectioning technique and sensitive liquid scintillation counting. The results of the gb diffusivity $P = \delta D_{gb}$ (δ: gb width, D_{gb}: gb diffusion coefficient) can be represented by the Arrhenius parameters $P_0 = 3{\cdot}27 \cdot 10^{13}$ m^3/s and $Q_{gb} = 168$ kJ/mol. Additionally gb diffusion was investigated in boron-doped (0·24 at%) Ni-rich Ni_3Al in the range from 882 to 1352 K yielding $P_0 = 1{\cdot}24 \cdot 10^{-12}$ m^3/s and $Q_{gb} = 187$ kJ/mol. The increase in the activation enthalpy Q_{gb} and the decrease of P upon boron-doping is explained by the segregation of B in Ni_3Al gbs, which may lead to an increase in the vacancy formation enthalpy and to a blocking of energetically favourable diffusion paths in the gbs. For comparison gb self-diffusion in pure Ni was remeasured yielding $Q_{gb} = 112$ kJ/mol. Ordering of the lattice and the preservation of ordering up to the gb planes, as predicted in Ni_3Al, therefore has a pronounced decelerating influence on gb diffusion, stronger than on bulk diffusion. Applying the semi-empirical relation of Borisov *et al.* (*Phys. Met. Metallogr.*, **17** (1964) 80) gb energies γ_{gb} were determined for arbitrary high angle gbs in pure and B-doped Ni_3Al, resulting in 915 and 870 mJ/m^2, respectively, at 1100 K. © 1996 Elsevier Science Limited

Keywords: A. intermetallics, nickel aluminides, based on Ni_3Al, B. diffusion, D. grain boundaries, F. trace element analysis.

1 INTRODUCTION

The ordered intermetallic compound Ni_3Al has attracted much attention as a potential high temperature material. The major difficulty in fabrication as a high temperature structural material is in its low ductility and brittle intergranular fracture at ambient temperature in polycrystalline state.[1,2] In conventional metals intergranular fraction is often associated with segregation of embrittling impurities, such as O, S and P, to grain boundaries (gbs). In contrast to that, the gbs of the ordered intermetallic compound Ni_3Al are basically clean and free of detectable impurities, as shown by AES analysis.[3,4] The intergranular fracture occurs in Ni_3Al without any appreciable segregation of impurities to the gbs. Therefore, the gb brittleness appears to be an intrinsic property of this compound.[4–8]

This feature, however, is not a property of $L1_2$ ordered alloys in general. For example Cu_3Au shows no intergranular brittleness. To understand this phenomenon it is reasonable to take a look at the ordering energy which has been identified as major factor controlling gb brittleness in ordered alloys. Calculations by Vitek *et al.*[9] have shown that the intrinsic brittleness of gbs in ordered compounds is directly related to the preference for certain chemical order. In strongly ordered $L1_2$ compounds, like Ni_3Al with an ordering energy of about 0·1 eV,[10] the ideal $L1_2$ structure is preserved up to the boundary plane without any relaxation of the atoms while in pure fcc metals and weakly ordered alloys (e.g. Cu_3Au) the distribution of atoms in the boundary region is more homogeneous and the chemical order is not necessarily preserved. In the former case this leads to the presence of columnar cavities in gbs which may serve as suitable nuclei for intergranular cracks.[9]

A very important finding associated with the intrinsic gb brittleness of the Ni_3Al compound is

*Present address: Hahn-Meitner-Institut GmbH, Glienicker Str. 100, D-14109 Berlin, Germany.

that alloying may have a dramatic effect on the ductility of this material. The first important parameter to take into consideration is the influence of the deviation from stoichiometry. Both nickel and aluminium segregate to the gbs when being in surplus in the bulk composition. Monte Carlo simulations[10] have shown that the impact of nickel segregation on the boundary structure is very different from that of aluminium segregation. The structural changes associated with the deviation from stoichiometry to Ni-rich compositions affect the crack nucleation and propagation along gbs. The cavities become much rarer and atoms are distributed more homogeneously so that gbs become chemically disordered. In contrast, in Al-rich Ni_3Al the segregation of Al may render the material even more brittle. Such an asymmetry occurs since it is energetically favourable to attain a surplus of Ni than a surplus of Al in the gb region, because the lattice parameters of Ni_3Al and Ni are very similar, while the lattice parameter of Al is significantly larger. A higher concentration of Ni in a gb may be achieved without any considerable mismatch with the bulk while this is not the case for Al. In fact, the Al-rich gbs have higher energy and are associated with a lower cohesive energy than Ni-rich gbs.[11] Nevertheless, the surplus of Ni alone is not sufficient for ductilization of polycrystalline Ni_3Al. Microalloying processes[3,12–15] have been used to alleviate the brittle intergranular fracture in Ni_3Al. Boron was found to be the most effective in improving the ductility of Ni_3Al. Boron dissolves interstitially in Ni_3Al,[16] occupying octahedral sites in the lattice, and shows a strong tendency to segregate to the gbs in an interstitial manner.[17] The boron dopants are most effective in improving the ductility and suppressing the brittle gb fracture in Ni-rich alloys.[3,15,18,19] The ductilization effect becomes less salient in Ni_3Al with higher aluminium concentrations. Liu *et al.*[3] have shown that the tensile ductility decreases and the tendency to gb fracture increases with the increase in aluminium concentration. AES studies of freshly fractured surfaces of B-doped Ni_3Al samples simultaneously traced out that the level of boron segregated to the gbs decreases with increasing Al concentration in Ni_3Al.[3]

The segregation of boron to the gbs, however, cannot be the only criterion since boron also segregates to the boundaries in Al-rich alloys which remain brittle. Many investigations to clarify the role of doped B atoms on ductilizing the Ni_3Al have been performed by means of experimental studies as well as theoretical treatments. To find additional criteria for the effect of ductilization, attention has been focused on the composition and state of ordering of the gb region.[20]

A possible explanation for this so called *boron-effect* was given by Vitek *et al.*[9] The authors suggested that the beneficial influence of boron on the boundary brittleness in Ni_3Al is at least twofold. First, the presence of boron in the interstitial sites at boundaries increases the gb cohesion, in particular in the presence of a surplus of Ni. Based on an electronic model to explain the effects of alloying elements on gb cohesion in metal[21] boron, which tends to segregate strongly in Ni_3Al gbs, enhances bonding between nickel atoms and results in an improvement of gb cohesion and reduction of the tendency towards brittle intergranular fracture.

Secondly, the interstitial segregation of boron atoms to the gbs simultaneously leads to an enhanced segregation of Ni to the boundaries. This leads to the same structural changes as in the case of large deviations from stoichiometry. Both these phenomena decrease the propensity to intergranular fracture.

All these facts indicate that alloy stoichiometry and microalloying strongly influence the gb chemistry and consequently the gb cohesion. However, a detailed atomistic mechanism for explaining the process of ductilization by the boron addition still remains uncertain.

Much effort has been devoted to investigate mechanical properties of this compound but experimental studies on the diffusion behaviour are relatively scarce and are almost lacking for the case of gb diffusion. To improve our understanding of the *boron-effect*, knowledge about the diffusion behaviour in the gbs in pure and in boron-doped Ni_3Al is of fundamental importance.

Apart from its technical importance, diffusion in the ordered $L1_2$-type intermetallic compound is also of fundamental scientific interest for its own sake. In pure metals such as Ni or in dilute substitutional Ni-alloys, self-diffusion can be considered to occur by random motion of vacancies without restriction. In ordered materials, however, a single exchange of an atom with a vacancy usually produces disordering. If the ordered lattice is to be retained it is necessary to invoke a more complex diffusion mechanism in the bulk and in principle also in gbs.

2 BULK SELF-DIFFUSION IN Ni_3Al

Before studying gb diffusion in a meaningful way, reliable information concerning the volume diffu-

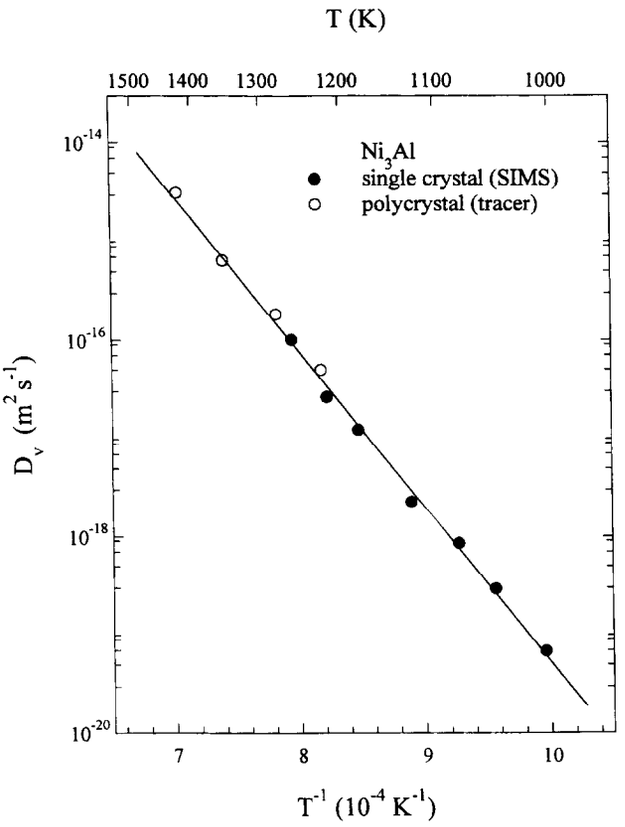

Fig. 1. Arrhenius plot of volume self-diffusion of Ni in Ni_3Al single and polycrystals.[25]

sion over a wide range of temperature is required. Volume self-diffusion of Ni in Ni_3Al was investigated by Hancock,[22] Bronfin *et al.*[23] and Shi *et al.*[24] in the temperature range above 1150 K. Investigating gb diffusion requires the knowledge of bulk diffusion coefficients especially at lower temperatures.

In a recent paper[25] we investigated therefore volume diffusion of Ni in Ni_3Al single (75·9 at% Ni) and polycrystals (75·2 at% Ni) in the temperature range from 1004 to 1422 K by applying tracer experiments by conventional serial sectioning and SIMS analysis using the isotopes ^{63}Ni and ^{64}Ni, respectively. The essential results of this investigations are:

(i) The temperature dependence of the diffusion coefficients D_v, Fig. 1, follows a perfect linear Arrhenius relation:

$$D_v = (3{\cdot}59^{+2{\cdot}59}_{-1{\cdot}50}) \cdot 10^{-4} \cdot \exp\left(-\frac{(303{\cdot}0 \pm 5{\cdot}3)\text{kJ/mol}}{RT}\right)\text{m}^2/\text{s} \quad (1)$$

This result differs from investigations of Hoshino *et al.*,[26] which reveal an enhanced diffusivity at very high and particularly at low temperatures resulting in a strongly curved Arrhenius plot. Possible reasons for this discrepancy were discussed.[25]

(ii) Ni diffusion occurs via nearest neighbour jumps of thermal vacancies in <110> direction in its own Ni sublattice (see Fig. 2).

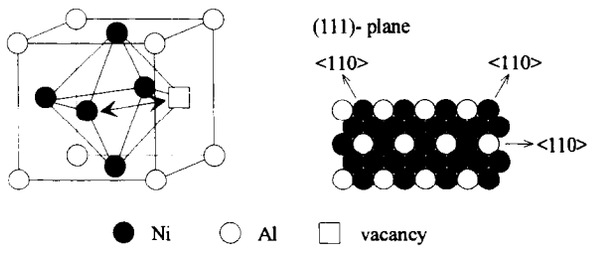

Fig. 2. Elementary diffusional jumps of Ni in Ni_3Al (nearest neighbour jumps in <110> direction).

Considering the fact that the volume diffusion of Ni in Ni_3Al shows only a very little variation of diffusion coefficients with composition[22,24,26] and that the interstitially dissolved boron dopants have no considerable influence on the volume diffusion behaviour,[26] the results from eqn (1) provide a good basis for investigating and evaluating quantitatively gb self-diffusion in Ni_3Al.

In this paper, we report on a study of gb diffusion in pure and B-doped Ni_3Al polycrystals. Diffusion penetration profiles were determined by a serial sectioning technique using a precision parallel grinding device. The low-energy β-decays of the ^{63}Ni tracer were detected by a liquid scintillation counter which provided the high counting efficiency required for detecting reliable gb diffusion profiles.

3 EXPERIMENTAL PROCEDURE

3.1 Specimen preparation

The investigation was performed on pure and B-doped polycrystalline Ni_3Al. Small grains, which are beneficial for the intended diffusion experiments, were achievable for the relative ductile boron-doped material. For that reason, one part of the doped Ni_3Al cast ingot was additionally cold worked with a deformation of about 10%. Chemical homogeneity of the alloys was generated by annealing at 1370 K for seven days. The actual compositions of the homogeneous ingots were determined by electron microprobe analysis using a well defined standard alloy as reference. The resulting compositions are given in Table 1.

Table 1. Sample compositions

Specimen	Composition (at% Ni)	Average grain diameter (μm)
Ni_3Al	75·1 ± 0·2	700
	76·9 ± 0·2	500
Ni_3Al + B	75·9 (+0·24 at% B) ± 0·2	500
Ni_3Al + B (cold-worked)	75·9 (+0·24 at% B) ± 0·2	200

The ingots were cut by spark erosion to rods with 7–8 mm in diameter. After cleaning and etching, cylindrical specimens were prepared by cutting the rod with a tungsten wire saw into 2–3 mm thick sections. The samples were polished using diamond paste and examined for optical flatness. After chemical etching the samples were subjected to a microstructural analysis by optical metallography. The average grain sizes of the different compositions, listed in Table 1, were found to be rather large but suitable for gb diffusion experiments. The polycrystals were preannealed at the same temperatures of the intended diffusion experiments in order to reduce the effect of defects in the surface layers on diffusion caused by the samples treatment and were slowly cooled down to room temperature. Furthermore, a stable gb structure for the current temperature was achieved.

3.2 Diffusion annealing and profile evaluation

The radiotracer ^{63}Ni was deposited in form of a diluted HCl solution onto the polished surface of the disc-like specimens. Diffusion anneals were performed at selected temperatures (882–1374 K). The temperature was measured with a calibrated PtRh–Pt thermocouple accurate to ±1K. All annealings were carried out in accordance to Harrisons[27] type B gb-diffusion kinetics. After annealing, the lateral surface of the cylindrical sample was removed mechanically by a special grinding device in order to avoid possible disturbing surface and radial diffusion effects. The determination of the diffusion penetration profiles was made by the radiotracer serial sectioning technique, measuring the average tracer concentration in thin sections parallel to the diffusion source as a function of the penetration depth. Because of the hardness and brittleness of the material the sectioning was performed using a precision parallel grinding device with special abrasive mylar foil. The thickness of each section was calculated from the mass reduction, measured with a microbalance, the diameter and the density of the Ni_3Al specimens.

The radioisotope ^{63}Ni (half-life about 100 years) decays by emission of electrons with the low energy of approximately 66 keV into the stable ^{63}Cu isotope. Different from the usually applied residual-activity measurement technique (Gruzin method[28]) in the case of ^{63}Ni, the activity of each section was detected directly with high efficiency by liquid scintillation counting. With regard to this, each abrasive mylar foil containing the removed Ni_3Al material was inserted into a 20 ml liquid scintillation vial and filled with a chemically aggressive scintillation cocktail. The main profit of this cocktail is the ability to dissolve the removed material and the abrasive Ni_3Al coating from the mylar foil. In contrast to the opaque coated original mylar foil, the now translucent foil does not disturb the liquid scintillation counting process providing in this way a counting efficiency of more than 90%. The section activity was measured with a Packard Tri Carb scintillation analyzer combined with an automatic sample changer.

The high counting efficiency allowed to significantly increase the detectable concentration range of the penetration profiles. In fact, despite of the coarse grained samples the gb diffusion related profiles were clearly observed even at temperatures as high as 1374 K.

4 RESULTS

The experiments were performed in the so-called type B kinetic regime in which diffusion along the gbs occurs simultaneously with volume diffusion from the gb into the adjacent bulk. Measurements in this regime, in which the condition $100\delta < \sqrt{D_v t}$ < grain size holds, yield the product $P = \delta D_{gb}$ of the gb-width ($\delta \approx 0{\cdot}5$ nm) and the gb self-diffusion coefficient D_{gb}. With regard to the presently applied sectioning technique this product can be evaluated from the slope of the concentration (c)–penetration (y) plot, following the solution of Suzuoka[29] for an instantaneous tracer source and using the expression[30]

$$P = \delta D_{gb} = 1{\cdot}308 \cdot \left(\frac{D_v}{t}\right)^{1/2} \left(-\frac{\partial \ln \bar{c}}{\partial y^{6/5}}\right)^{-5/3} \quad (2)$$

For $\beta > 10^4$ and with minor changes for values $\beta < 10^2$ or $10^2 < \beta\ 10^4$. D_v represents the diffusion coefficient in the bulk, t is the annealing time and $\bar{c}$ the mean tracer concentration in a section of the diffusion profile at depth y parallel to the sample surface. The quantity

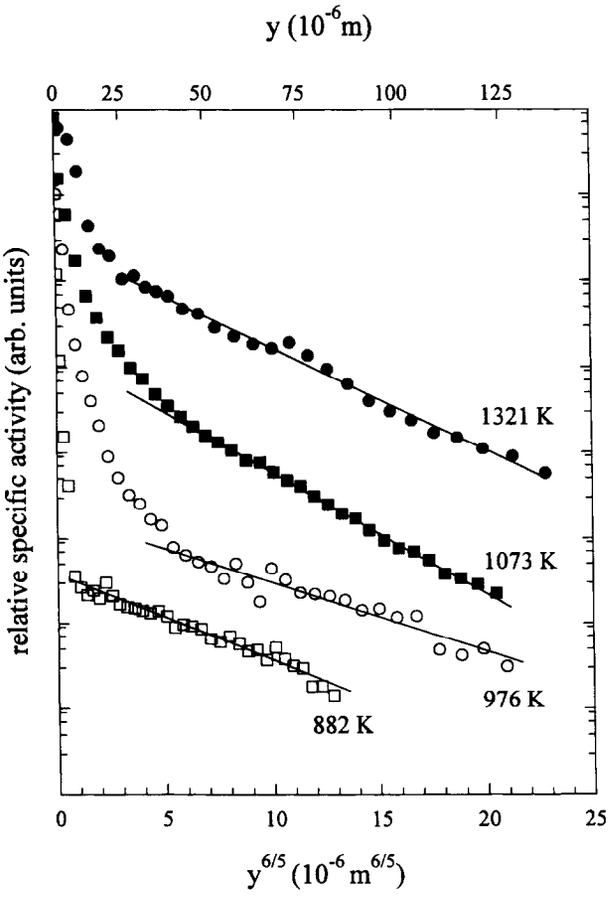

Fig. 3. Penetration profiles of grain boundary diffusion of ^{63}Ni in $Ni_{75\cdot1}Al_{24\cdot9}$.

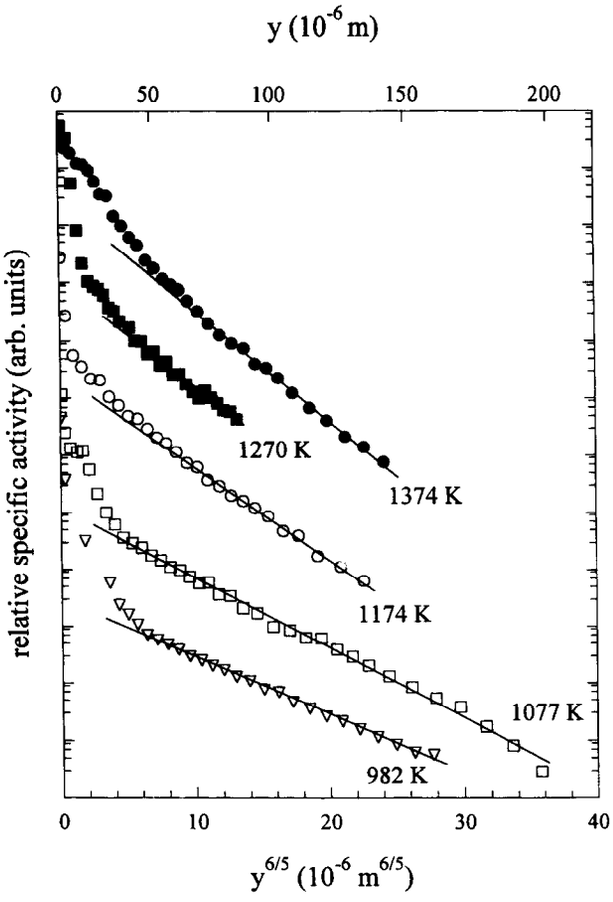

Fig. 4. Penetration profiles of grain boundary diffusion of ^{63}Ni in $Ni_{76\cdot9}Al_{23\cdot1}$.

$$\beta = \frac{\delta D_{gb}}{2D_v\sqrt{D_v t}}$$

specifies the shape of the diffusion profile in the vicinity of the gb. The validity of eqn (2) is confined to $\beta > 10$, which restricts the extension of the investigations to high temperatures.

Figures 3 and 4 show the measured gb diffusion profiles in the pure Ni_3Al material. The steep initial high-concentration part close to the surface corresponds to the superposition of bulk diffusion from the free surface and gb diffusion whereas (in terms of eqn (2)) the linear low-concentration part at deep penetrations can be attributed to gb diffusion in type B kinetics. The observed linear decrease in the relative specific activity over about two orders of magnitude allows a reliable calculation of $P = \delta D_{gb}$. Applying eqn (2), the required bulk self-diffusion coefficients D_v of Ni in Ni_3Al were calculated from eqn (1).

4.1 Grain boundary diffusion of Ni in pure Ni_3Al

Experiments were performed in an alloy of almost stoichiometric composition and in a Ni-rich compound (Table 1). Previous[22,26] and extensive recent investigation[24] have shown that Ni diffusion in Ni_3Al is almost independent from deviations of the stoichiometry. It is therefore justified to use data of D_v from eqn (1) for the calculation of $P = \delta D_{gb}$ in both alloys. The results of P and the related experimental quantities are summarized in Tables 2 and 3. Figure 5 presents the Arrhenius plot of $P(T)$ in both Ni_3Al alloys. The good agreement between the two sets of results is remarkable. Though it was not intended *a priori* to measure $P(T)$ in dependence on concentration some valuable information is obtained in this respect (see below).

Within the limits of the experimental error all data follow one straight Arrhenius line which is described by

Table 2. Results of grain boundary diffusion of ^{63}Ni in $Ni_{75\cdot1}Al_{24\cdot9}$

T/K	t/s	D_v/m^2s^{-1}	β	$P=\delta D_{gb}/m^3s^{-1}$
1321	32400	$3\cdot75 \cdot 10^{-16}$	43	$1\cdot15 \cdot 10^{-19}$
1073	259200	$6\cdot38 \cdot 10^{-19}$	2565	$1\cdot70 \cdot 10^{-21}$
976	604800	$2\cdot18 \cdot 10^{-20}$	79008	$4\cdot01 \cdot 10^{22}$
882	604800	$4\cdot08 \cdot 10^{-22}$	$3\cdot15 \cdot 10^{6}$	$3\cdot93 \cdot 10^{-23}$

$$P = \delta D_{gb} = (3{\cdot}27^{+2{\cdot}46}_{-1{\cdot}40}) \cdot 10^{-13} \cdot \exp\left(-\frac{(168{\cdot}0 \pm 5{\cdot}1)\text{kJ/mol}}{RT}\right)\text{m}^3/\text{s} \quad (3)$$

This result represents gb self-diffusion behaviour in general large angle gbs of pure nickel-rich Ni_3Al.

4.2 Grain boundary diffusion of Ni in boron-doped Ni_3Al

To obtain information about the influence of boron segregation in Ni_3Al gbs on the diffusion process, gb self-diffusion was measured in a boron-doped Ni_3Al alloy ($Ni_{75.9}Al_{24.1}$ + 0·24 at% B) of a Ni composition within the range of the investigated pure Ni_3Al material. Polycrystals with an average grain diameter of 500 and 200 μm were used, originating from the same as cast alloy after cold working of one part of the ingot. Reliable gb diffusion profiles were measured in the temperature range from 882 to 1251 K. The profiles are shown in Figs 6(a) and 7 for the coarse and smaller grain size, respectively. Two further experiments were performed at even higher temperatures which still reveal gb diffusion tails, see insert in Fig. 6(b). However, the corresponding values of β are too small (about 2) to comply with eqn (2). Instead, these profiles represent first of all bulk diffusion in the boron-doped alloy, Fig. 6(b), as shown by the usual Gaussian plot of ln$c$ versus y^2 of the first parts of the profiles. The bulk diffusion coefficients resulting from this linear parts: D_v = 7·48 · 10^{-16} m^2/s (T = 1352 K) and D_v = 2·01 · 10^{-16} m^2/s (T = 1279 K) agree nicely with those in pure Ni_3Al, eqn (1). Doping of Ni_3Al with 0·24 at% B therefore does not significantly affect the bulk self-diffusion behaviour. This finding is in fairly good agreement with the measurements of Hoshino *et al.*[26] and allows us to use D_v data from eqn (1) to evaluate the gb diffusion parameter P in the boron-doped Ni_3Al alloy. As expected, the different grain size of the materials has no influence on the results of $P(T)$, however, the quality of the profiles in the gb diffusion dominated parts is better for samples of smaller grain size, see Fig. 7 in comparison to Fig. 6(a). The initial parts of several profiles reveal a fairly broad transition range from the bulk to the gb dominated part. This feature might be related to a small gb migration of certain grains in the samples during the diffusion anneal.[31,32] Such an effect was recently quantitatively investigated in Nb.[33] It does not disturb the correct evaluation of $P(T)$ provided that the profiles are detected to large penetration depths, where the linear relation of ln$c$ versus $y^{6/5}$ stems from diffusion along stationary gbs.

Table 3. Results of grain boundary diffusion of ^{63}Ni in $Ni_{76.9}Al_{23.1}$

T/K	t/s	D_v/m^{2}s^{-1}	β	$P=\delta D_{gb}$/m^{3}s^{-1}
1374	18000	1·09 · 10^{-15}	12	1·17 · 10^{-19}
1270	36000	1·23 · 10^{-16}	60	3·15 · 10^{-20}
1174	36000	1·19 · 10^{-17}	779	1·21 · 10^{-20}
1077	176400	7·24 · 10^{-19}	4136	2·15 · 10^{-21}
982	518400	2·74 · 10^{-20}	51720	3·41 · 10^{-22}

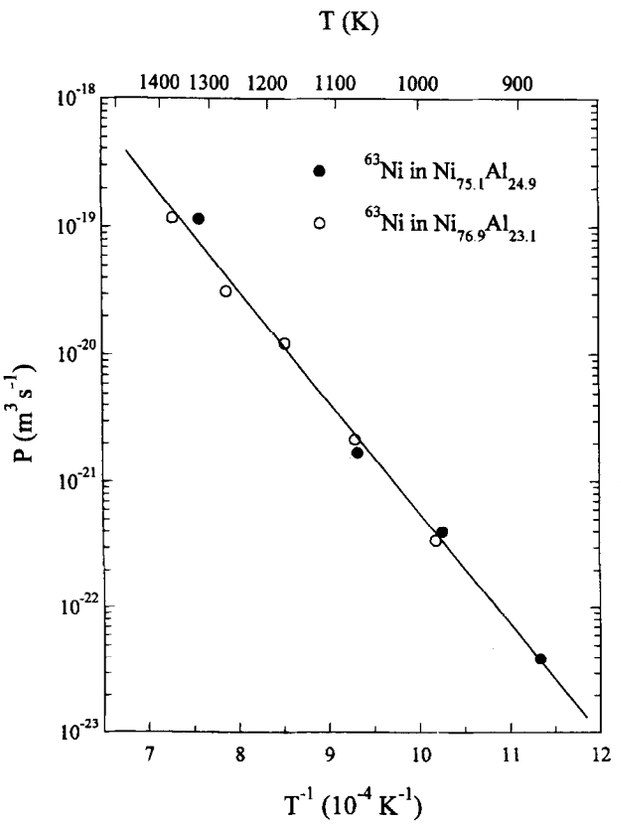

Fig. 5. Arrhenius plot of grain boundary self-diffusion of ^{63}Ni in Ni_3Al (nearly stoichiometric and Ni-rich composition).

All relevant quantities are summarized in Table 4. Figure 8 shows the corresponding Arrhenius presentation of $P(T)$. As observed in pure Ni_3Al, the Arrhenius plot is linear and is characterized by

$$P = \delta D_{gb} = (1{\cdot}24^{+1{\cdot}03}_{-0{\cdot}56}) \cdot 10^{-12} \cdot \exp\left(-\frac{(187{\cdot}0 \pm 5{\cdot}4)\text{kJ/mol}}{RT}\right)\text{m}^3/\text{s} \quad (4)$$

The activation enthalpy of gb self-diffusion in the pure Ni_3Al material is therefore smaller by about 19 kJ/mol than that in B-doped Ni_3Al of similar deviation from stoichiometry to the Ni-rich side.

In Table 5 the Arrhenius parameters are compared to those of gb self-diffusion in pure Ni,

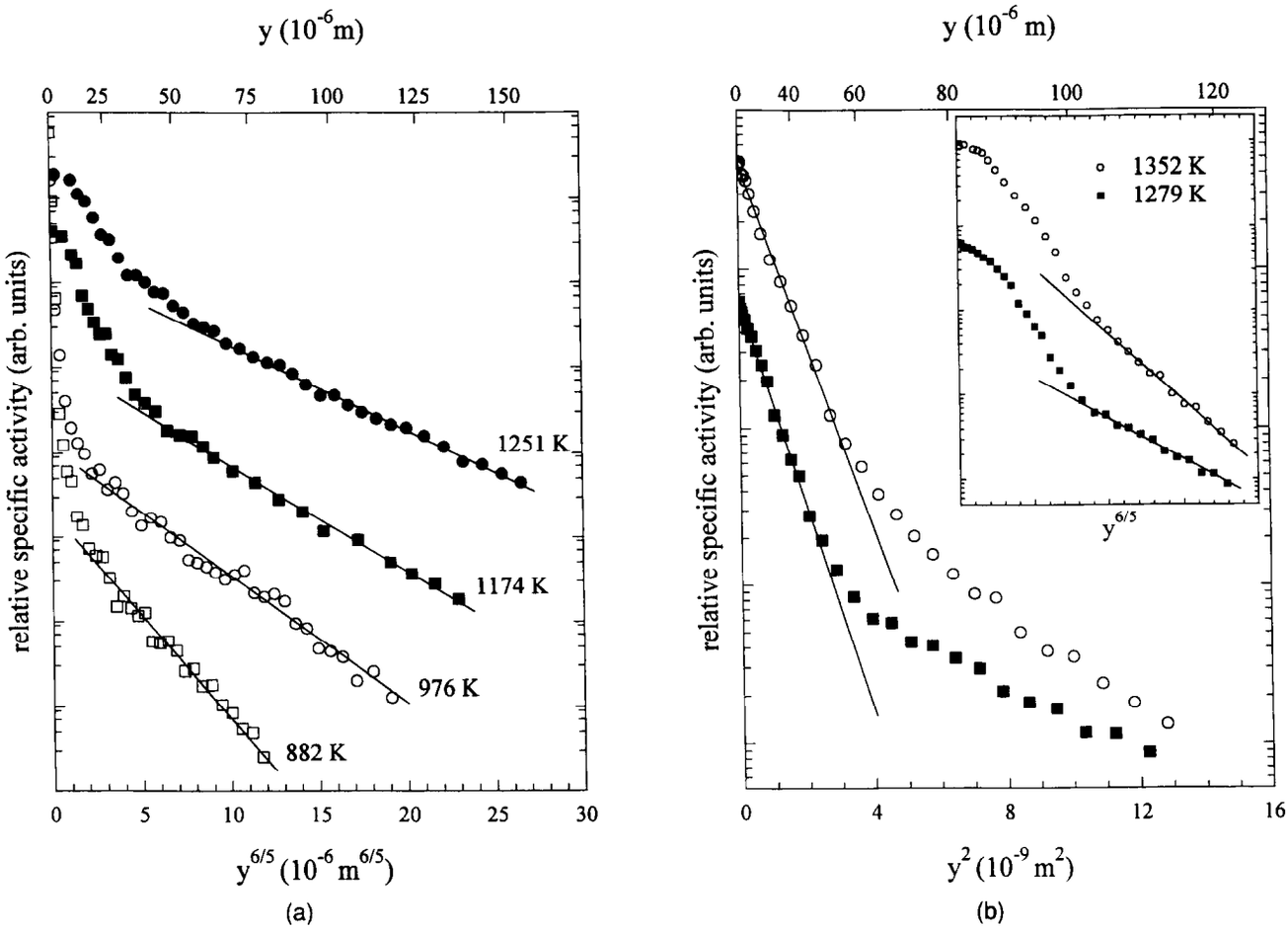

Fig. 6. (a) Penetration profiles of grain boundary diffusion of ^{63}Ni in boron-doped Ni_3Al (grain-size ≈ 500 μm). (b) Penetration profiles of grain boundary diffusion of ^{63}Ni in boron-doped Ni_3Al at elevated temperatures showing contributions from diffusion in the volume and along grain boundaries.

which was recently reinvestigated by us in true type B-kinetic conditions.[34]

5 DISCUSSION

The Suzuoka solution[29] of the gb diffusion problem was applied to calculate the parameter P in gbs of the ordered compound Ni_3Al. This solution is based on the Fisher model,[35] which assumes a grain boundary of small constant width ($\delta \approx 0{\cdot}5$ nm) and the bulk and gb diffusion coefficients independent of position. These requirements are most likely fulfilled in the highly ordered Ni_3Al, because the ideal $L1_2$ structure is preserved up to the gb plane.[10] In general, the evaluation of the gb diffusivity may become more sophisticated in ordered compounds if broader relaxation zones with changing composition between the gb core and the bulk are formed.[36]

Our recent remeasurement of Ni self-diffusion in Ni_3Al poly- and single crystals[25] revealed a perfectly linear Arrhenius relation, eqn (1), from which D_v is calculated in order to determine $P = \delta D_{gb}$ from eqn (2). In view of the presently measured gb diffusion profiles it seems most likely that the low temperature enhancement of D_v, as measured by Hoshino *et al.*,[26] stems from short circuit diffusion processes. Polycrystalline samples of similar grain size as in the present gb diffusion study were applied in ref. 26.

Gb diffusion was determined in samples of an almost stoichiometric (75.1 at%) and Ni-rich (76.9 at%) composition. The results of P are presented in Fig. 5. Within the limits of error both sets of P-data follow the same Arrhenius relation, eqn (3). Monte Carlo calculations revealed a Ni segregation to gbs in Ni-rich Ni_3Al.[10] This surplus of Ni, however, obviously has no significant influence on the Ni diffusivity. Similar to the situation in the bulk[37] it is reasonable to assume that also in the gbs vacant sites are preferentially formed in Ni positions and that jumps of Ni atoms occur via such Ni positions. In the Ni-rich alloy a certain

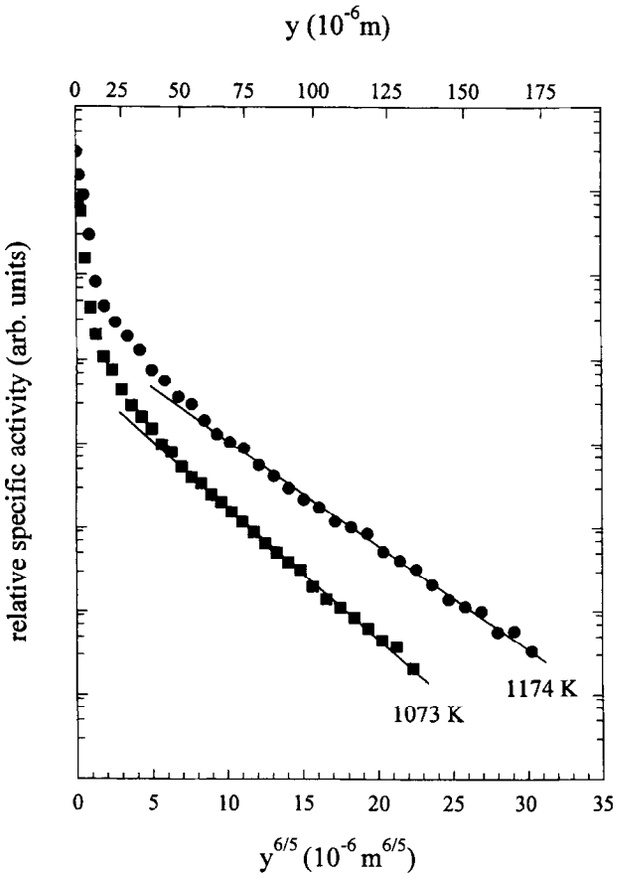

Fig. 7. Penetration profiles of grain boundary diffusion of ^{63}Ni in boron-doped Ni_3Al (grain-size ≈ 200 μm).

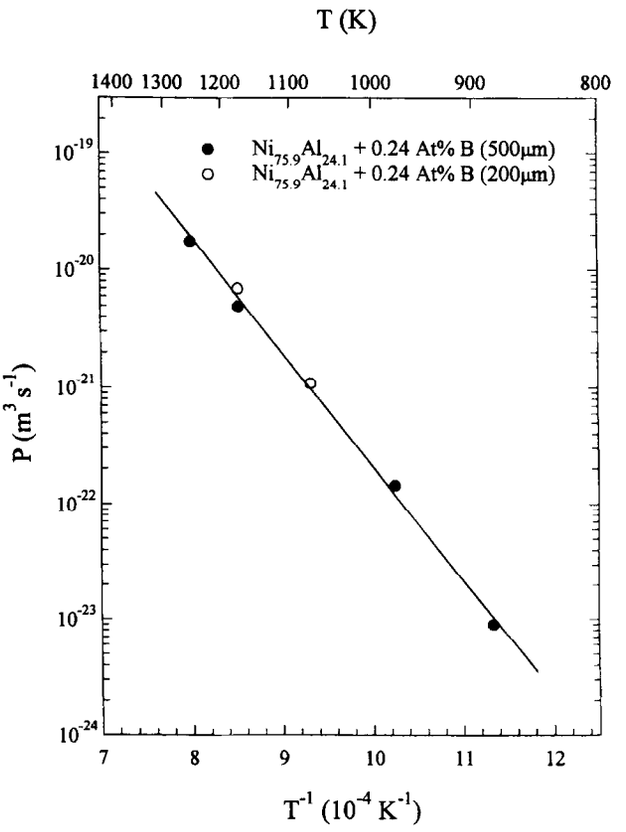

Fig. 8. Temperature dependence of grain boundary diffusion of ^{63}Ni in boron-doped Ni_3Al.

Table 4. Grain boundary diffusion of ^{63}Ni in boron-doped $Ni_{75.9}Al_{24.1}$

T/K	t/s	D_v/m^2s^{-1}	β	$P=\delta D_{gb}$/m^3s^{-1}
1251	522000	$8.01 \cdot 10^{-17}$	17	$1.75 \cdot 10^{-20}$
1174	522000	$1.19 \cdot 10^{-17}$	83	$4.97 \cdot 10^{-21}$
1174	259200	$1.19 \cdot 10^{-17}$	164	$6.95 \cdot 10^{-21}$
1073	259200	$6.38 \cdot 10^{-19}$	2105	$1.09 \cdot 10^{-21}$
976	604800	$2.18 \cdot 10^{-20}$	28608	$1.45 \cdot 10^{-22}$
882	604800	$4.08 \cdot 10^{-22}$	707700	$9.03 \cdot 10^{-24}$

compositional disorder of the gb structure is expected due to the calculated Ni segregation. As the majority of the atomic positions of the gb consists of Ni atoms a small Ni surplus obviously remains ineffective in the present study in which diffusion in arbitrary large angle gbs was investigated. Computer simulations of the structure and composition of gbs were made so far for individual symmetrical tilt gbs of Ni_3Al.[9,10,17]

At present very little is known about the diffusion in gbs of ordered compounds. As a first step a comparison with the atomic mobility in gbs of the pure metal seems to be meaningful. We therefore remeasured gb self-diffusion in polycrystals of pure Ni in true type-B diffusion kinetics.[34] The resulting Arrhenius parameters $P_0 = 1.71 \cdot 10^{-15}$ m^3/s and $Q_{gb} = 112.1$ kJ/mol, Table 5 and Fig. 9, differ considerably from those in Ni_3Al. The comparison between pure Ni and Ni_3Al shows that the ratio of the activation enthalpies for bulk diffusion $Q_v^{Ni}/Q_v^{Ni_3Al} = 0.92$ is not far from unit,[25,38] while for gb diffusion the activation enthalpy in the compound is significantly larger than in pure Ni, $Q_{gb}^{Ni}/Q_{gb}^{Ni_3Al} = 0.67$. It is a very reasonable result that in an ordered compound like Ni_3Al, (where diffusion proceeds via thermal vacancies only[25]), diffusion activation enthalpies are larger than in the pure base metal. The comparatively small increase of Q_v in the compound Ni_3Al with respect to Ni results from the fact that in the Ll_2-structure Ni atoms migrate in their own sublattice. Ordering is not effected by this process. Furthermore, vacancies are formed predominantly in the Ni sublattice and the vacancy formation enthalpy in Ni_3Al[37,39] (≈ 1.9 eV) is very similar to that in pure Ni[40] (1.78 eV).

The situation is obviously different for gb diffusion. Due to the high ordering energy, gb atoms in Ni_3Al can be regarded as uniquely attached to either the one or the other grain, if the ideal Ll_2-structure is practically preserved on each side of

Table 5. Arrhenius parameter of gb self-diffusion of ^{63}Ni in pure and boron-doped Ni_3Al and in pure Ni. The activation enthalpy for bulk self-diffusion Q_v is listed for comparison. The marked data result from: *[25], §[34], #[38]

	P_0/m^3s^{-1}	Q_{gb}		Q_v	
		eV/atom	kJ/mol	eV/atom	kJ/mol
Pure Ni_3Al	$(3{\cdot}27^{+2{\cdot}46}_{-1{\cdot}40}) \cdot 10^{-13}$	1·74 ± 0·05	168·0 ± 5·1	3·14 ± 0·05	303·0 ± 5·3*
Boron-doped Ni_3Al	$(1{\cdot}24^{+1{\cdot}03}_{-0{\cdot}56}) \cdot 10^{-12}$	1·94 ± 0·06	187·0 ± 5·4	—	—
Pure Ni	$(1{\cdot}71^{+0{\cdot}34}_{-0{\cdot}28}) \cdot 10^{-15}$	1·16 ± 0·02	112·1 ± 1·6§	2·88	278#

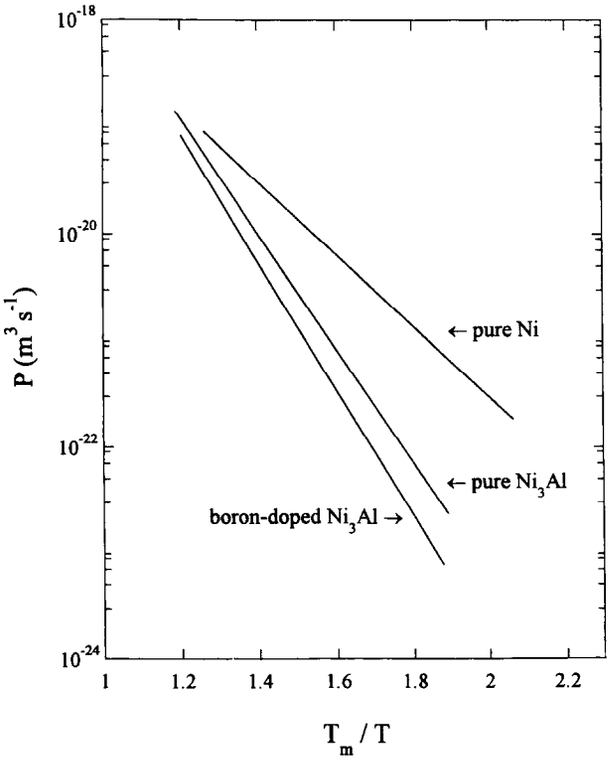

Fig. 9. Comprehensive Arrhenius plot of Ni grain boundary self-diffusion in pure and boron-doped Ni_3Al in comparison with Ni grain boundary self-diffusion in pure Ni.[34]

the gb plane. The chemical order is the principal factor in controlling the energy of the system and is dominating the gb structure. The lack of relaxation in the boundary region and the preservation of chemical order produces geometrical restrictions in the atomic jumps and impedes vacancy formation and migration in Ni_3Al boundaries resulting in a fairly large activation enthalpy and low mobility as compared to pure Ni, Fig. 9. This fact is supported by the ratios

$$Q_{gb}^{Ni_3Al}/Q_v^{Ni_3Al} = 0{\cdot}55 \text{ and } Q_{gb}^{Ni}/Q_v^{Ni} = 0{\cdot}40$$

for the activation enthalpies of gb and bulk self-diffusion in both materials. The ratio of 0·4 is typical for self-diffusion in pure closed packed metals, e.g. Ag.[41] In view of the similarity of Q_v in both materials it is the large value of $Q_{gb}^{Ni_3Al}$ which yields to the enhanced ratio in Ni_3Al.

The temperature dependence of Ni diffusion in grain boundaries of boron-doped Ni_3Al is presented in Fig. 9 in comparison with the results in pure Ni_3Al and in pure Ni. The diffusivity in the doped alloy is about 2–3 times lower than in pure Ni_3Al, which clearly demonstrates the effect of boron segregation. Calculations have shown that B segregates at interstitial positions in the gb.[17] Gb cohesion is improved by this due to an enhanced bonding between the Ni atoms.[21] From this bonding effect an increase in the formation enthalpy of vacancies at Ni sites in the boundary is expected. Furthermore, the dissolution of B atoms at certain sites in the gb structure will impede or even block Ni atom jumps which are energetically favourable in pure Ni_3Al gbs. Both effects result in an increase of the effective diffusion activation enthalpy and in a reduction of the mobility as compared to pure Ni_3Al. As the present experiments show, Fig. 9 and Table 5, the interference of boron atoms is remarkable but not dramatic. The observations are in accordance with the more general experience that impurity segregation reduces the mobility of the solvent atoms along gbs.[42]

The present results allow the estimation of the gb energy in pure and boron-doped Ni_3Al, and in pure Ni for comparison, by applying the semi-empirical relationship of Borisov *et al.*[43] The basic postulate in this relation is that the Gibbs free energy ΔG_{gb} for activating atom-vacancy jumps in the gb, to a first approximation, is reduced with respect to atom-vacancy activation free energy in the bulk, ΔG_v, by the absolute gb energy γ_{gb}:

$$\gamma_{gb} \approx \Delta G_v - \Delta G_{gb}$$

Relating to Borisov *et al.*, Gupta[44] derived the following expression for the average energy of large angle gbs at temperature T(K):

$$\gamma_{gb} = \frac{kT}{2a^2} \ln\left(\frac{D_{gb}}{D_v}\right)$$

$$= \frac{1}{2a^2 N_A} \left(RT \ln\left(\frac{D_{gb}^0}{D_v^0}\right) + (Q_v - Q_{gb})\right) \qquad (5)$$

where a is the lattice parameter (0·356 nm for Ni_3Al[45]) and $D_{gb} = P/\delta$, D_v are the diffusion coefficients along gbs and in the lattice, respectively, assuming $\delta = 0{\cdot}5$ nm. N_A is Avogadro's number and D^0 and Q are the corresponding Arrhenius parameters.

The reliability of the Borisov relationship has been checked several times in the literature in different metals and dilute substitutional alloy[46–48] yielding fairly good agreement with available experimental data of γ_{gb}, despite the semi-empirical character of eqn (4).

Applying the present results, Table 5, to eqn (5) γ_{gb} was calculated for the temperature range between 900 and 1400 K as depicted in Fig. 10. Roughly, γ_{gb} amounts to about 900 mJ/m^2. The detailed inspection reveals a smaller gb energy in the boron-doped than in the pure Ni_3Al material, which is meaningful, since segregation of B atoms reduces the energy of Ni_3Al gbs. As segregation decreases with increasing temperature, γ_{gb} increases as well, approaching γ_{gb} of pure Ni_3Al, which shows a negligible temperature dependence only within the experimental uncertainty. Obviously the entropy term in γ_{gb} is very small in Ni_3Al gbs due to the high ordering. The clearly negative temperature dependence of γ_{gb} in pure Ni on the other hand corresponds to a comparatively larger entropy contribution in the relaxed gb structure of pure Ni. This behaviour and the smaller values of γ_{gb} (at least for $T \geq 1100$ K) are reasonable results.

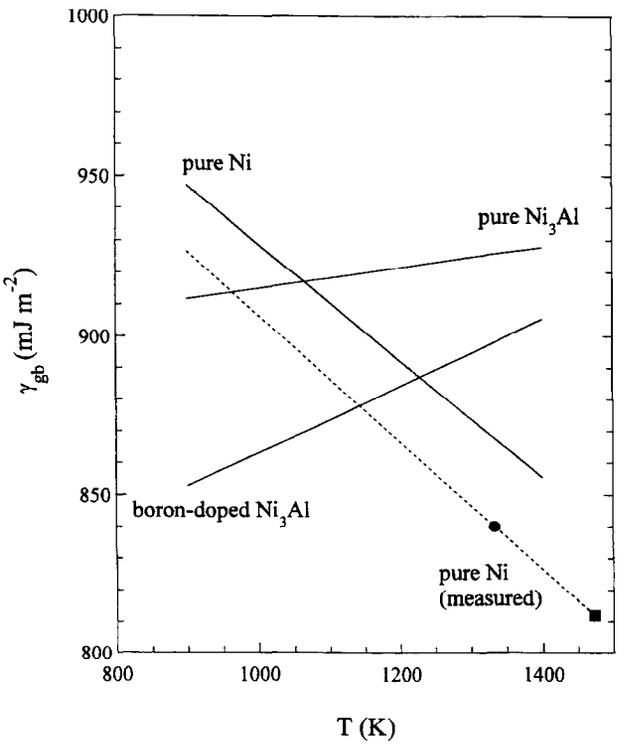

Fig. 10. Grain boundary energy γ_{gb} of large angle gbs in pure and boron-doped Ni_3Al and in pure Ni obtained by applying the Borisov *et al.* relation[43] to the present diffusion results (full lines). Directly measured values of γ_{gb} in pure Ni are shown for comparison: ● Murr *et al.*;[49] ■Muschik.[50]

Experimentally γ_{gb} was determined in random gbs in pure Ni by Murr[49] at $T = 1333$ K and by Muschik[50] at $T = 1473$ K, see full symbols in Fig. 10. Regarding the assumptions involved in the Borisov relation and in the experimental determination of γ_{gb} the present results of Fig. 10 in Ni and Ni_3Al are satisfying.

6 SUMMARY AND CONCLUSIONS

Ni diffusion along arbitrary large angle gbs of pure Ni_3Al is much smaller than in pure Ni, resulting in a comparatively larger increase of the activation enthalpy $Q_{gb}^{Ni_3Al}$ with respect to pure Ni than it is observed for the corresponding bulk diffusion behaviour of both materials. The predicted preservation of ordering of the lattice up to the gb plane therefore has a larger impact on vacancy formation and migration of Ni atoms in the gb core than in lattice positions of Ni_3Al as compared to pure Ni.

The doping of Ni_3Al with 0·24 at% B and the segregation of B decreases Ni gb diffusion by a factor of 2–3 and increases Q_{gb} slightly with respect to pure Ni_3Al. This results from an increase in gb cohesion and Ni–Ni atom bonding upon boron-doping. The segregation of B at interstitial positions of the gb structure may furthermore block otherwise energetically favourable diffusion paths along gbs. The reduction of mobility as compared to pure Ni_3Al is not dramatic and in accordance with the experience of a reduced solvent atom mobility along gbs caused by impurity segregation.

Grain boundary energies γ_{gb} determined from the present diffusion results with the Borisov *et al.* relation[43] amount to about 915 mJ/m^2 in Ni_3Al. γ_{gb} is smaller in B-doped Ni_3Al gbs and reveals a positive temperature dependence approaching γ_{gb} of pure Ni_3Al due to the change of B segregation with temperature. For pure Ni on the other hand γ_{gb} decreases with increasing temperature. The entropy contribution to the gb energy obviously is larger in Ni gbs than in gbs of the ordered Ni_3Al compound.

The observed effect of boron-doping on the gb diffusivity and gb energy is not extraordinarily large. A straightforward link to the previously

detected change in the fracture mode from brittle, intergranular to ductile, transgranular upon B-doping is not directly obvious.

ACKNOWLEDGEMENTS

The authors are grateful to Professor G. Gottstein and Dr C. Y. Ma for supplying Ni_3Al alloys.

REFERENCES

1. Meyers, D. E. & Ardell, A. J., *Acta Metall. et Mater.*, **41** (1993) 2601.
2. Sizek, H. W. & Gray, G. T., *Acta Metall. et Mater.*, **41** (1993) 1855.
3. Liu, C. T., White, C. L. & Horton, J. A., *Acta metall.*, **33** (1985) 213.
4. Ogura, T., Hanada, S., Masumoto, T. & Izumi, O., *Metall. Trans.*, **16A** (1985) 441.
5. Takasugi, T., Masahashi, N. & Izumi, O., *Acta metall.*, **33** (1985) 1247.
6. Takasugi, T., George, E. P., Pope, D. P. & Izumi, O., *Scripta metall.*, **19** (1985) 551.
7. Takasugi, T., Nagashima, M. & Izumi, O., *Acta metall.*, **38** (1990) 747.
8. Liu, C. T., *Scripta Metall. et Mater.*, **25** (1991) 1231.
9. Vitek, V. & Chen, S. P., *Scripta Metall. et Mater.*, **25** (1991) 1237.
10. Yan, M., Vitek, V. & Ackland, G. J., *Ordered Intermetallics—Physical Metallurgy and Mechanical Behaviour*, Eds C. T. Liu *et al.*, Kluwer Academic Publishers, Dordrecht, 1992, p. 335.
11. Chen, S. P., Voter, A. F. & Srolovitz, D. J., *Scripta metall.*, **20** (1986) 1389.
12. Aoki, K. & Izumi, O., *Trans. Japan Inst. Metals*, **19** (1978) 203.
13. Qian, X. R. & Chou, Y. T., *Mater. Lett.*, **6** (1988) 157.
14. Qian, X. R. & Chou, Y. T., *J. Mater. Sci.*, **27** (1992) 1036.
15. Choudhury, A., White, C. L. & Brooks, C. R., *Scripta metall.*, **20** (1986) 1061.
16. Fischer, B., Ittermann, B., Diehl, E., Dippel, R., Ergezinger, K. H., Frank, H.-P., Jäger, E., Seelinger, W., Sulzer, G., Ackermann, H., Stöckmann, H.-J. & Bohn, H. G., *Ann. Phys.*, **47** (1990) 659.
17. Farkas, D. & Rangarajan, V., *Acta metall.*, **35** (1987) 353.
18. Choudhury, A., White, C. L. & Brooks, C. R., *Acta Metall. et Mater.*, **40** (1992) 57.
19. White, C. L. & Stein, D. F., *Metall. Trans.*, **9A** (1978) 13.
20. Baker, I., Schulson, E. M. & Michael, J. R., *Phil. Mag.*, **B57** (1988) 379.
21. Messmer, R. P. & Briant, C. L., *Acta metall.*, **30** (1982) 457.
22. Hancock, G. F., *phys. stat. sol. (a)*, **7** (1971) 535.
23. Bronfin, M. B., Bulatov, G. S. & Drugova, I. A., *Fiz. metall.*, **40** (1975) 363.
24. Shi, Y., Frohberg, G. & Wever, *phys. stat. sol (a)*, **152** (1995) 361.
25. Frank, S., Södervall, U. & Herzig, Chr., *phys. stat. sol. (b)*, **191** (1995) 45.
26. Hoshino, K., Rothman, S. J. & Averback, R. S., *Acta metall.*, **36** (1988) 1271.
27. Harrison, L. G., *Trans. Faraday Soc.*, **57** (1961) 1191.
28. Gruzin, P. L., *Dokl. Akad. Nauk. SSSR*, **86** (1952) 289.
29. Suzuoka, T., *Trans. Jap. Inst. Metals*, **2** (1961) 25.
30. Kaur, I., Mishin, Y. M. & Gust, W. *Fundamentals of Grain and Interphase Boundary Diffusion*, John Wiley & Sons Ltd, Chichester, 1995, p. 59.
31. Mishin, Y. M. & Razumovskii, I. M., *Acta Metall. et Mater.*, **40** (1992) 839.
32. Glaeser, A. M. & Evans, J. V., *Acta metall.*, **34** (1986) 1545.
33. Köppers, M., Mishin, Y. M. & Herzig, Chr., *Acta Metall. et Mater.*, **42** (1994) 2859.
34. Frank, S. & Herzig Chr., to be published.
35. Fisher, J. C., *J. Appl. Phys.*, **22** (1951) 74.
36. Mishin, Y. M. & Yurovitskii, I. V., *Phil. Mag.*, **A64** (1991) 1239.
37. Badura, K. A., Dissertation, Universität Stuttgart, 1995.
38. Maier, K., Mehrer, H., Lessmann, E. & Schüle, W., *phys. stat. sol. (b)*, **78** (1976) 689.
39. Badura, K. A. & Schäfer, H. E., *Verh DPG*, **7** (1995) 1458.
40. Schäfer, H. E., *phys. stat. sol. (a)*, **102** (1987) 47.
41. Sommer, J. & Herzig, Chr., *J. Appl. Phys.*, **72** (1992) 2758.
42. Kaur, I., Mishin, Y. M. & Gust, W., *Fundamentals of Grain and Interphase Boundary Diffusion*, John Wiley & Sons Ltd, Chichester, 1995, p. 412.
43. Borisov, V. T., Golikov, V. M. & Scherbedinsky, G. V., *Phys. Met. Metallogr.*, **17** (1964) 80.
44. Gupta, D., *Metall. Trans.*, **8A** (1977) 1431.
45. Aoki, K. & Izumi, O., *phys. stat. sol. (a)*, **32** (1975) 657.
46. Pelleg, J., *Phil. Mag.*, **14** (1966) 594.
47. Gupta, D., *Phil. Mag.*, **33** (1976) 189.
48. Gupta, D., Research Report, IBM Research Division, New York, 1987, p. 52.
49. Murr, L. E., Horilev, R. J. & Lin, W. N., *Phil. Mag.*, **22** (1970) 515.
50. Muschik, T., Dissertation, Universität Stuttgart, 1988, p. 156.